J Therm Anal Calorim (2010) 99:117–122
DOI 10.1007/s10973-009-0486-5

Thermal change of organic light-emitting ALQ3 thin films

Mei-Han Wang · Takayuki Konya · Masahiro Yahata · Yutaka Sawada · Akira Kishi · Takayuki Uchida · Hao Lei · Yoichi Hoshi · Li-Xian Sun

Japan Symposium 2008
© Akadémiai Kiadó, Budapest, Hungary 2009

Abstract A series of Alq3 thin films with the thicknesses of 50, 100, and 200 nm was deposited on Si substrates at room temperature using the thermal evaporation method. The thermal crystallization process of Alq3 thin films, especially 50 nm thick films, was successfully examined using high-temperature X-ray diffraction (HT-XRD) with the in-plane scan mode. Film thickness, density, and changes in surface roughness while heating were determined using X-ray reflectometry (XRR). The decreased density and increased surface roughness, which were accompanied by sublimation, indicate the instability of the Alq3 film. Thus, thermal instability is a major factor for device failure.

Keywords Alq3 thin film · Thermal crystallization · High-temperature X-ray diffraction · Thermal change · X-ray reflectometry

M.-H. Wang · M. Yahata · Y. Sawada (✉) · T. Uchida · H. Lei · Y. Hoshi
Center for Hyper Media Research, Tokyo Polytechnic University, 1583 Iiyama, Atsugi, Kanagawa 243-0297, Japan
e-mail: sawada@nano.t-kougei.ac.jp

T. Konya · A. Kishi
Rigaku Corporation, 3-9-12 Matsubara, Akishima, Tokyo 196-8666, Japan

L.-X. Sun
Materials and Thermochemistry Laboratory, Dalian Institute of Chemical Physics, Chinese Academy of Sciences, 457 Zhongshan Road, Dalian 116023, China

Y. Sawada
Department of Industrial Chemistry, Graduate School of Engineering, Tokyo Polytechnic University, 1583 Iiyama, Atsugi, Kanagawa 243-0297, Japan

Introduction

Organic light-emitting devices (OLEDs) are currently under intense investigation for applications in next generation display technologies. OLEDs are heterojunction devices where organic active layers, which behave as thin solid films, are incorporated into devices. In 1987, Tang and VanSlyke first reported an efficient OLED using tris-(8-hydroxyquinoline)aluminum (Alq3) as the electron-transport layer and light-emitting material [1]. Since then Alq3 has become a standard electro-luminescent material for the devices.

Despite displaying excellent device characteristics, full realization of OLED technology has been hampered due to a lack of device stability. OLEDs incorporating Alq3 suffer from device degradation due to localized chemical failure and an intrinsic degradation in performance with time [2]. Many articles have reported that water vapor is more severe chemical failure of Alq3 than oxygen [3–7]. The reaction of Alq3 with water has been interpreted to form 8-hydroxyquinoline (8-Hq), which reacts with O_2 to produce non-emissive polymer. The hydrolysis of an Alq3 material in a wet atmosphere has also been verified using sample-controlled thermogravimetry (SCTG) [8] by the present authors. Encapsulating an OLED can eliminate water and oxygen, but thermal instability of Alq3 induced by the Joule heating effect during operation remains. Hence, thermal crystallization of amorphous Alq3 films and other thermal changes should be examined as a function of temperature and time, but thermal analysis of thin films is difficult due to the minute specimen sample.

Xu et al. have applied variable temperature tapping mode atomic force microscopy (VT-AFM) to visualize thermally activated degradation pathways in Alq3 thin films (56 nm), where thermal crystallization is determined by a

pronounced morphological change [9]. Jian et al. have also adopted AFM to study Alq3 films (150 nm) deposited on a sapphire plate at various substrate temperatures [10]. However, the AFM method offers local topographic information obtained only for the optimal location on a sample surface and protrusions, which appeared on the image, may be insufficient to draw conclusions about thermal crystallization. X-ray diffraction methods are most suitable for structural evaluations of materials. Kajimoto et al., a group who studies the decay process of this luminescent material, have reported that 520 nm thick Alq3 films display clear diffraction peak after annealing for 11 h at 423 K using XRD with Bragg–Brentano geometry [11]. However, a thickness greater than 500 nm is far from industrial applications. The conventional X-ray techniques are, in general, not applicable to organic thin film due to strong diffractions and scatterings from the substrates. In contrast, the XRD method in the in-plane scan mode is a powerful technique to determine the phase transition in a film, even for a single layered LB film [12].

X-ray reflectometry (XRR) is an ideal means to measure the properties of surfaces and interfaces as thickness, density, and interface information are provided even from fairly complex thin film stacks. Recently, this technique has been applied to OLEDs and polymer films [13–15]. Lee et al. investigated thermal degradation of OLED multilayers (LiF/Alq3/NPB/CuPc/ITO/SiO_2 on glass) by XRR and reported that the thermally induced degradation process of OLED multilayers had undergone several evolutions due to thermal expansion of NPB, intermixing between NPB, Alq3, and LiF layers, dewetting of NPB on CuPc and crystallization of NPB and Alq3.

X-ray reflectometry is a simple and easy technique to analyze the relatively weak interactions between X-rays and the atoms in solids, so they can typically be described in terms of perturbations. This greatly simplifies the mathematical description of the X-ray scattering process and permits the process to be quantitative modeled with relative ease. The normal output of an XRR experiment exhibits a regime of nominal total external reflection when the specular angle is less than the critical angle [16]:

$$\theta_C \approx \sqrt{2\delta} = \sqrt{\frac{\lambda^2 r_0 \rho}{\pi}}, \tag{1}$$

where δ is the real part of the X-ray refractive index expressed in terms of the classical electron radius r_0, λ the X-ray wavelength, and ρ the electron density. Above the critical angle, the intensity decreases with an inverse fourth-power dependence on the scattering angle. Simultaneously, the intensity of X-rays reflected by thin films or layer stacks vary periodically in response to changes in the incidence angle. These periodic variations arise from the interference of radiation reflected by each of the interlayer interfaces.

Herein, the thermal stability of amorphous Alq3 thin films was analyzed using high-temperature X-ray diffraction (HT-XRD) with the in-plane scan mode and XRR. Our data using the XRD method provides evidence that thermal crystallization of amorphous Alq3 occurs upon heating, especially for 50 nm thick thin films, and explains the degradation of device lifetime caused by thermal change.

Experimental

Deposition of Alq3 thin films

Alq3 was purchased from OHJEC Corporation and used as supplied without further purification. The silicon substrates were commercial polished wafers with a (100) orientation. The silicon substrates (15×15 mm^2) were heated at 823 K in air for 30 min, and then degreased with acetone, rinsed with propanol, dried in a vacuum, and irradiated by UV light. Amorphous Alq3 films with thicknesses of 50, 100, and 200 nm were deposited at room temperature by vacuum thermal evaporation method. The system was evacuated using a turbo-molecular pump to a background pressure of $\sim 8 \times 10^{-4}$ Pa. The crucible was heated using a basket-shaped tungsten wire. Alq3 film thickness was monitored by a crystal oscillator with a fixed deposition rate of 6 nm/min. The as-deposited films were directly transferred from the vacuum chamber into glove box and inserted into a sealed transfer vessel to minimize degradation caused by exposure to the atmosphere.

High-temperature X-ray diffraction (HT-XRD) with the in-plane scan mode

The thermal crystallization process was monitored using a dome type HT-XRD (SmartLab 9 kW, Rigaku) in the in-plane scan mode diffraction method. The in-plane scan mode, namely the diffraction planes which are perpendicular to the film surface, is an excellent technique to detect the diffraction for ultra thin films. Alq3 thin films were heated to various annealing temperatures (423, 433, and 443 K) in high-purity N_2 with a flow rate of 100 mL/min. For an in-plane XRD measurement, a parallel monochromatic X-ray beam operating at 45 kV and 200 mA was incident to the sample at an angle of 0.2°. The scattered X-ray intensity was monitored as a function of 2θ angle with the in-plane geometry. Data were collected in a range of $2\theta = 5$–30° at intervals of 0.1° with a scan speed of 0.8°/min using a scintillation counter.

X-ray reflectometry

X-ray reflectometry analyses were performed using a Rigaku SmartLab high-resolution diffractometer operated in a 2θ geometry, which registers lattice planes parallel to the substrate surface. X-ray through beam conditioner is a monochromatic Cu $K_{\alpha 1}$ incident. The reflected incident beam was conditioned by a variable slit before being detected by a scintillation counter. XRR intensities were recorded over an angular range from $2\theta = 0.2°$ (below the critical angle) until all the intensity oscillations due to film thickness were damped out by the effects of interfacial roughness, before $2\theta = 10°$. The film thickness, density, and apparent roughness during annealing were determined based on Parratt's formalism [17].

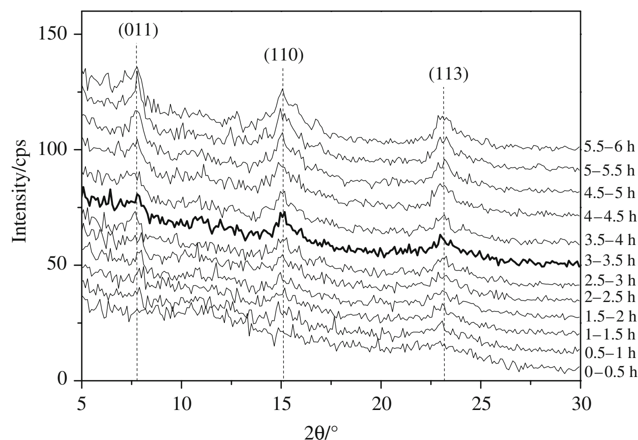

Fig. 2 HT-XRD spectra of an Alq3 film with the thickness of ~200 nm annealed at 433 K

Results and discussion

Thermal crystallization

Figure 1 shows the XRD spectra of the as-deposited Alq3 films with different thicknesses. Two halos appeared on all spectra, suggesting an amorphous-like structure. The diffraction intensity increased with film thickness, which agrees with the finding that evaporated Alq3 films at room temperature are amorphous-like and composed of meridional isomers of Alq3 molecules [18, 19].

Thermal crystallization from the amorphous phase was detected for a 200 nm thick Alq3 film after annealing for 8 h at 423 K. Increasing the temperature (433 K) reduced the crystallization time to 3 h (Fig. 2). The three strongest diffraction peaks in the XRD spectrum are ascribed to α phase of Alq3 according to Cambridge Structural Database. For a thinner film (100 nm thick), the period for crystallization was reduced to 2 h at the same annealing temperature (433 K). However, as shown in Fig. 3, when the 100-nm thick film was annealed at 443 K the thermal crystallization process was completed within 30 min.

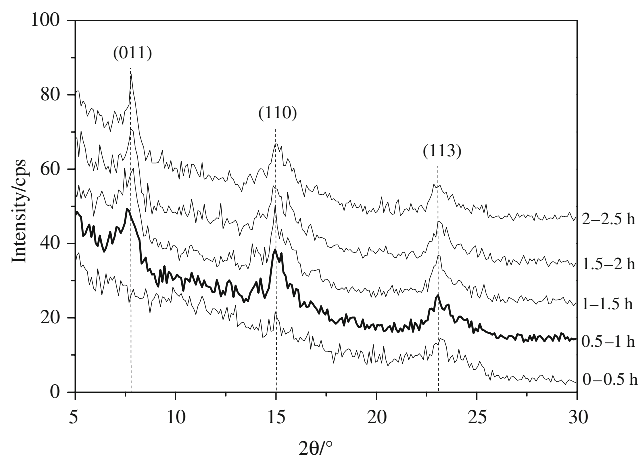

Fig. 3 HT-XRD spectra of an Alq3 film with the thickness of ~100 nm annealed at 443 K

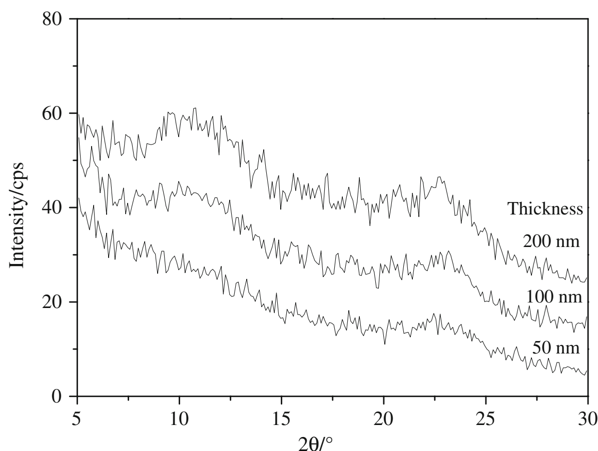

Fig. 1 XRD spectra of the as-deposited Alq3 films with different thicknesses

Thermal crystallization of a 50-nm thick film is crucial for understanding the thermal effect for real devices because this thickness is comparable to OLEDs (~40–50 nm [20]). Figure 4 shows the HT-XRD spectra of a 50-nm thick film annealed at 443 K. Very weak diffraction peaks appeared after annealing 2 h, which decreased and eventually disappeared. This behavior is attributed to the sublimation of the specimen.

Thickness, density, and roughness

A model structure consisting of (a) the silicon substrate, (b) an interfacial SiO_2 oxide, and (c) the Alq3 layer was used as the initial structure to calculate a trial reflectometry

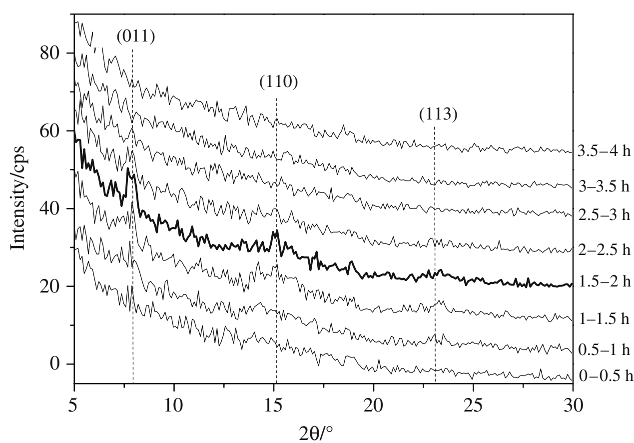

Fig. 4 HT-XRD spectra of an Alq3 film with the thickness of ~50 nm annealed at 443 K

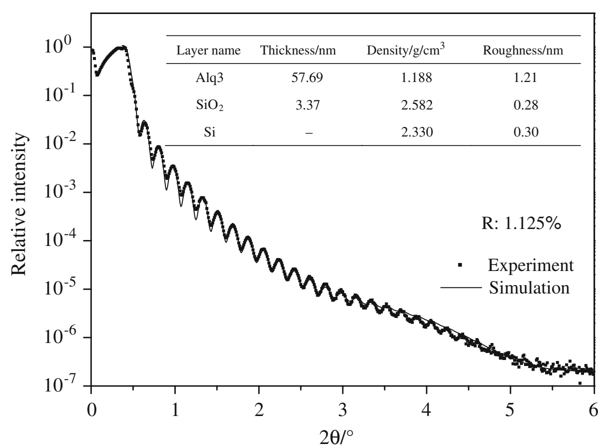

Fig. 5 X-ray reflectometry curve of the as-deposited Alq3 film with the thickness of ~50 nm on Si along with the simulation curve

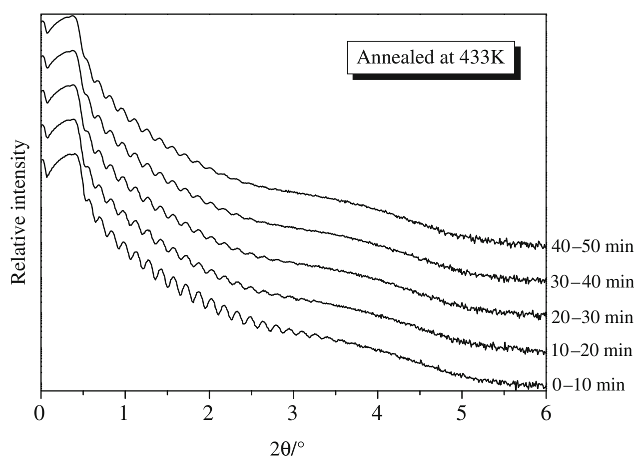

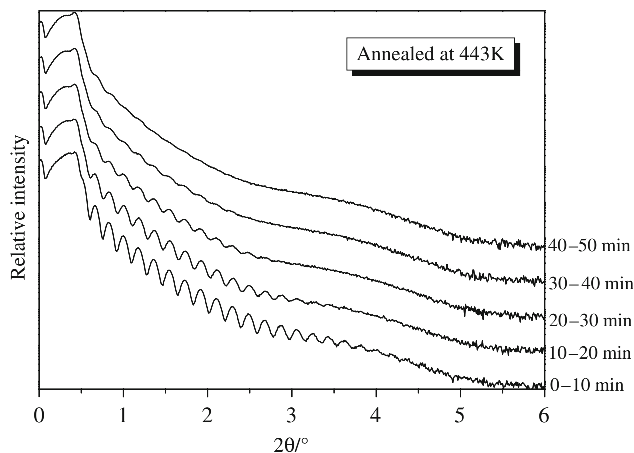

Fig. 6 X-ray reflectometry curves of Alq3 films with the thickness of ~50 nm on Si annealed at 433 and 443 K

curve. The thickness, density, and roughness of the Alq3 layers were then varied according to a genetic algorithm to minimize the difference between the observed and calculated X-ray scans. Figure 5 depicts the model structure, which generated the calculated curves with the best fit to the experimental data for the as-deposited Alq3 thin film (~50 nm). The non-linear least square fitting of the experimental XRR curves with the profiles calculated using the relatively simple model above resulted in very good agreement between theory and experiment. The reliability of the fitting was estimated by *R*. The reliability factor *R* was 1.125%, which was as good as the allowable value. The thickness, density, and roughness of Alq3 layer were 57.69 nm, 1.188 g/cm^3, and 1.21 nm, respectively. The small difference in the electron densities of Si and SiO_2 made the fitting process insensitive to the structural details of the oxide; hence, in these samples, the oxide thickness and Si/SiO_2 interfacial roughness were kept constant.

In order to investigate the thickness, density, and roughness change of Alq3 film during heating, an XRR scan was collected every 10 min. Figure 6 shows the experimental XRR curves obtained from a Alq3 film (~50 nm) annealed at 433 and 443 K. The intensity of interference fringe decreased with the annealing time, and almost disappeared after 40 min at 443 K, indicating that the roughness significantly increased during thermal crystallization. Each XRR scan was simulated using the above structure mode. Figure 7 shows the density and thickness changes of the Alq3 films (~50 nm) as a function of annealing time at 433 and 443 K. The estimated standard deviation errors of the density change with annealing time for the films annealed at 433 and 443 K were 0.0128 and 0.0020, respectively. The film density gradually decreased with heating time when annealed at 433 K. In contrast, the density remarkably decreased after 30 min when annealed at 443 K. This decreased density is attributed to the sublimation of Alq3. As the film thickness remained nearly constant during the heating process, the decrease in film density suggests the Alq3 film became porous. Figure 8

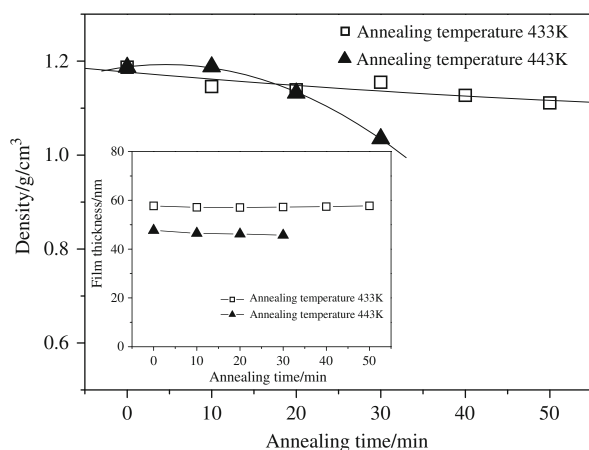

Fig. 7 Density and thickness changes of Alq3 films annealed at different temperatures as a function of annealing time

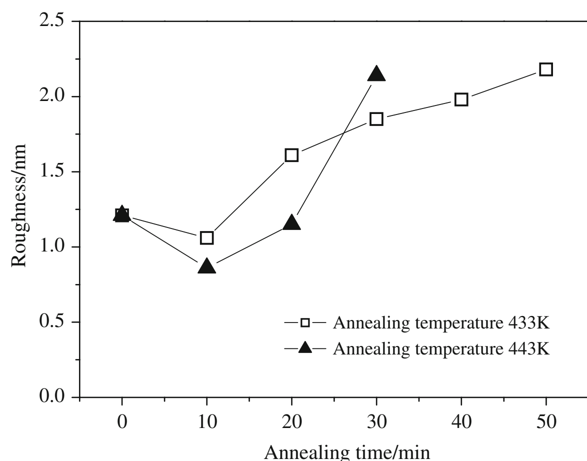

Fig. 8 Roughness change in Alq3 films annealed at different temperatures as a function of annealing time

shows the roughness change of the Alq3 films ($\sim$50 nm). The figure depicts that the roughness initially decreased, but then increased. A glass transition temperature of Alq3 film has been reported [9] near 403–413 K; thus, the roughness after the decrease is ascribed to the glass transition. The increased roughness after the glass transition is interpreted by the simultaneous thermal crystallization and sublimation process.

Although more measurements are necessary to fully understand these observations, these results clearly demonstrate that amorphous Alq3 thin films are unstable during heating. Simultaneous thermal crystallization and sublimation lead to a decrease in density, but increase in roughness. Moreover, these results confirm that XRR is a highly effective analysis method to evaluate the thermal change of small molecular organic thin films.

Conclusions

High-temperature X-ray diffraction with an in-plane scan mode is successfully employed to systematically visualize the thermally induced crystallization of Alq3 thin films. Films with thicknesses of 100 and 200 nm display clear diffraction peaks, which are ascribed to the α-phase of Alq3. For 50 nm thick films, which are compatible with OLEDs, weak diffraction peaks appear after annealing for 2 h at 443 K. These results suggest HT-XRD in the in-plane scan mode is a novel, but excellent thermal analysis for time-dependent crystallization of nm thick organic amorphous thin films. Film thickness, density, and surface roughness changes of Alq3 thin films during heating can be elucidated by XRR measurement. The film thickness remains nearly constant during the heating process. However, the film density gradually decreases and the surface roughness obviously increases with heating time. Hence, the thermal instability of Alq3 films is considered as a significant factor for device failure.

Acknowledgements The authors thank the Ministry of Education, Culture, Sports, Science and Technology (MEXT) for financial support for our High-Tech Research Center Project entitled Development of Flexible Transparent Light Emitting Display Devices.

References

1. Tang CW, VanSlyke SA. Organic electroluminescent diodes. Appl Phys Lett. 1987;51:913–5.
2. Aziz H, Popovic ZD. Degradation phenomena in small-molecule organic light-emitting devices. Chem Mater. 2004;16:4522–32.
3. Xu MS, Xu JB. Nanoscale study on origins of the bright clusters in/on moisture-exposed tris(8-hydroxyquinoline) aluminum thin films. Synth Met. 2004;145:177–82.
4. Xu MS, Xu JB, Lou EZ, Xie Z. Nanoscale investigation on nature of dark hole in moisture-exposed tris(8-hydroxyquinoline) aluminum thin films. Chem Phys Lett. 2003;374:656–60.
5. Papadimitrakopoulos F, Zhang XM, Thomsen DL III, Higginson KA. A chemical failure mechanism for aluminum(III) 8-hydroxyquinoline light-emitting devices. Chem Mater. 1996;8:1363–5.
6. Papadimitrakopoulos F, Zhang XM. Environmental stability of aluminum tris(8-hydroxyquinoline) (Alq3) and its implications in light emitting devices. Synth Met. 1997;85:1221–4.
7. Higginson KA, Zhang XM, Papadimitrakopoulos F. Thermal and morphological effects on the hydrolytic stability of aluminum tris(8-hydroxyquinoline) (Alq3). Chem Mater. 1998;10:1017–20.
8. Wang MH, Sawada Y, Saito K, Horie S, Uchida T, Ohtsuka M, et al. Thermal change of Alq3, tris(8-hydroxyquinolinato) aluminum(III) studied by TG and XRD-DSC. J Therm Anal Calorim. 2007;89:363–6.
9. Xu MS, Xu JB. Visualization of thermally-activated degradation pathways of tris(8-hydroxyquinoline) aluminum thin films for electroluminescence application. Thin Solid Film. 2005;491: 317–22.
10. Jian ZA, Luo YZ, Chung JM, Tang SJ, Kuo MC, Shen JL, et al. Effects of isomeric transformation on characteristics of Alq3 amorphous layers prepared by vacuum deposition at various substrate temperatures. J Appl Phys. 2007;101:123708-1–6.

11. Kajimoto N, Manaka T, Iwamoto M. Decay process of a large surface potential of Alq3 films by heating. J Appl Phys. 2006; 100:053707-1–6.
12. Takahashi S, Taniguchi M, Omote K, Wakabayashi N, Tanaka R, Yamagishi A. First observation of in-plane X-ray diffraction arising from a single layered inorganic compound film by a grazing incidence X-ray diffraction system with a conventional laboratory X-ray source. Chem Phys Lett. 2002;352:213–9.
13. Lee YJ, Lee H, Byun Y, Song S, Kim JE, Eom D, et al. Study of thermal degradation of organic light emitting device structures by X-ray scattering. Thin Solid Film. 2007;515:5674–7.
14. Andrew N, Benjamin WM, James O, Celesta F, Keith MM, Patrick GH, et al. X-ray and neutron reflectometry study of glow-discharge plasma polymer films. Langmuir. 2006;22:453–8.
15. Mobus M, Karl N. The growth of organic thin films on silicon substrates studied by X-ray reflectometry. Thin Solid Film. 1992;215:213–7.
16. Matyi RJ, Hatzistergos MS, Lifshin E. X-ray reflectometry analyses of chromium thin films. Thin Solid Film. 2006;515: 1286–93.
17. Parratt LG. Surface studies of solids by total reflection of X-rays. Phys Rev. 1954;95:359–69.
18. Curry RJ, Gillin WP, Clarkson J, Batchelder DN. Morphological study of aluminum tris(8-hydroxyquinoline) thin films using infrared and Raman spectroscopy. J Appl Phys. 2002;92:1902–5.
19. Kaji H, Kusaka Onoyama YG, Horii F. CP/MAS 13C NMR characterization of the isomeric states and intermolecular packing in tris(8-hydroxyquinoline) aluminum(III) (Alq3). J Am Chem Soc. 2006;128:4292–7.
20. Uchida T, Mimura T, Kaneta S, Ichihara M, Ohtsuka M, Otomo T. Transparent organic light-emitting devices fabricated by Cs-incorporated RF magnetron sputtering deposition. Jpn J Appl Phys. 2005;44:5939–42.